

Highly Entangled Ground States in Tripartite Qubit Systems

Beat Röthlisberger, Jörg Lehmann, D. S. Saraga, Philipp Traber, and Daniel Loss
Department of Physics, University of Basel, Klingelbergstrasse 82, CH-4056 Basel, Switzerland
(Dated: May 30, 2018)

We investigate the creation of highly entangled ground states in a system of three exchange-coupled qubits arranged in a ring geometry. Suitable magnetic field configurations yielding approximate GHZ and exact W ground states are identified. The entanglement in the system is studied at finite temperature in terms of the mixed-state tangle τ . By generalizing a conjugate gradient optimization algorithm originally developed to evaluate the entanglement of formation, we demonstrate that τ can be calculated efficiently and with high precision. We identify the parameter regime for which the equilibrium entanglement of the tripartite system reaches its maximum.

PACS numbers: 03.67.Mn, 03.65.Ud

Entangled quantum systems have been the focus of numerous theoretical and experimental investigations [1–3]. In particular, entanglement has been identified as the primary resource for quantum computation and communication [4]. Compared to the case of a bipartite system, multipartite entanglement exhibits various new features. Notably, there are two different equivalence classes of genuine three-qubit entanglement [3], the representatives being any one of the two maximally entangled Greenberger-Horne-Zeilinger (GHZ) states [2] $|\text{GHZ}^\pm\rangle = (|\uparrow\uparrow\uparrow\rangle \pm |\downarrow\downarrow\downarrow\rangle)/\sqrt{2}$ on the one hand, and the W state [3] $|\text{W}\rangle = (|\uparrow\uparrow\downarrow\rangle + |\uparrow\downarrow\uparrow\rangle + |\downarrow\uparrow\uparrow\rangle)/\sqrt{3}$ on the other. The ability to realize both representatives in real physical systems is thus of high importance in the study of genuine tripartite entanglement. Particularly interesting is the GHZ state, as it represents the strongest quantum correlations possible in a system of three qubits. Furthermore, it is equivalent to the three-qubit cluster state used in one-way quantum computation [5]. It is favorable to obtain the GHZ and W states as the eigenstate of a suitable system, rather than by engineering them using quantum gates. In this Letter, we demonstrate the possibility of obtaining approximate GHZ and exact W states as the ground state (g.s.) of three spin-qubits in a ring geometry coupled via an anisotropic Heisenberg interaction. The use of quantum gates is therefore not required. Rather, the desired states are achieved merely by cooling down to sufficiently low temperatures. We state all our results in terms of the exchange coupling strengths in order to keep our proposal open to a broad set of possible implementations of the qubits. We remark that, while Heisenberg models have been studied frequently in the context of entanglement [6] (also with respect to entangled eigenstates [7]), this is the first time that highly entangled states are reported as the non-degenerate g.s. of three exchange-coupled qubits. Our study inevitably involves the issue of quantifying entanglement [8–12]: At finite temperatures, the mixing of the g.s. with excited states forces us to evaluate a mixed-state entanglement measure (EM) in order to study the entanglement in the system meaningfully. Computationally, this is a rather formidable

task. We generalize a numerical scheme that has originally been developed to compute the entanglement of formation (EOF) [10, 13]. Our scheme can be used to evaluate *any* mixed-state EM defined as a so-called convex roof [14].

Model.— We assume that three spins \mathbf{S}_i , with $S = 1/2$, are located at the corners $i = 1, 2, 3$ of an equilateral triangle lying in the xy -plane. Their interaction is described by the anisotropic Heisenberg Hamiltonian

$$H = -J_{xy} \sum_{i=1}^3 (S_i^x S_{i+1}^x + S_i^y S_{i+1}^y) - J_z \sum_{i=1}^3 S_i^z S_{i+1}^z + H_Z, \quad (1)$$

where $\mathbf{S}_4 = \mathbf{S}_1$. Here, J_{xy} and J_z are the in- and out-of-plane exchange coupling constants, respectively, and $H_Z = \sum_{i=1}^3 \mathbf{b}_i \cdot \mathbf{S}_i$ denotes the Zeeman coupling of the spins \mathbf{S}_i to the externally applied magnetic fields \mathbf{b}_i at the sites i [15]. We now seek a configuration of \mathbf{b}_i 's yielding a highly entangled GHZ- or W-type *ground state*. Finite-temperature effects will then be studied in a second step.

Ground-state properties.— We first consider isotropic exchange couplings, i.e., $J_{xy} = J_z \equiv J$. For $\mathbf{b}_i = 0$, we naturally find two fourfold-degenerate eigenspaces due to the high symmetry of the system. For $J > 0$, i.e., ferromagnetic coupling, the ground-state quadruplet is spanned by the two GHZ states $|\text{GHZ}^\pm\rangle$, the W and the spin-flipped W state. Appropriately chosen magnetic fields allow one, however, to split off an approximate GHZ state from this degenerate eigenspace. To identify the optimal field geometry, we first observe that the two states $|\text{GHZ}^\pm\rangle$ have the form of a tunnel doublet. If we thus find a set of \mathbf{b}_i 's, which, in the classical spin system, results in precisely two degenerate minima for the configurations $\uparrow\uparrow\uparrow$ and $\downarrow\downarrow\downarrow$ with an energy barrier in between, quantum tunneling will yield the desired states. In order to single out exactly the two directions perpendicular to the xy -plane, the magnetic fields must be in-plane, be of the same strength, and sum to zero. This immediately implies that successive directions of the fields must differ by an angle of $2\pi/3$ from each other. We choose the fields to point radially outwards, although any other config-

uration possessing the required symmetry is equivalent. However, this setup is experimentally most feasible, e.g., by placing a bar magnet below the center of the sample (in the case of a solid state implementation). In order to favor parallel spin configurations we consider the regime where $J \gg b$, $b = |\mathbf{b}_i|$ being the Zeeman energy. We may thus assume that for given mean spherical angles $\bar{\vartheta}$ (zenith) and $\bar{\varphi}$ (azimuth), the orientation of each spin will deviate from these values only by a small amount. Expanding the classical energy $E_c(\bar{\vartheta}, \bar{\varphi})$ corresponding to Eq. (1) to second order in these deviations and minimizing with respect to them under the constraint that they separately sum to zero yields:

$$E_c \approx -\frac{(b/J)^2}{8}(3 + \cos 2\bar{\vartheta}) + \frac{(b/J)^3}{24} \sin(3\bar{\varphi}) \sin^3 \bar{\vartheta}. \quad (2)$$

This expression is minimal for $\bar{\vartheta} = 0$ and $\bar{\vartheta} = \pi$, representing the desired configurations. The paths in $\bar{\vartheta}$ with lowest barrier height connecting these two minima are found for values of $\bar{\varphi} = -\pi/6 + 2\pi n/3 \pmod{2\pi}$, $n = 0, 1, 2$, reflecting the rotational symmetry of the system. The corresponding barrier height is approximately given by $[(b/J)^2 - (b/J)^3/6]/4$ [16].

Next we return to the quantum system. The Hamiltonian (1) with isotropic exchange coupling J and radial magnetic field can be diagonalized exactly. Expanding for $b/J \ll 1$, the overlap probabilities of the exact ground state $|0\rangle$ with $|\text{GHZ}^+\rangle_{\text{l.u.}}$ and the exact first excited state $|1\rangle$ with $|\text{GHZ}^-\rangle_{\text{l.u.}}$, respectively, are identical to second order and are given by $|\langle \text{GHZ}^+ | 0 \rangle|^2 = |\langle \text{GHZ}^- | 1 \rangle|^2 \approx 1 - \frac{1}{3}(b/J)^2$ ('l.u.' indicates that the states are equivalent to GHZ states via local unitary transformations). The associated energy splitting is given by $\Delta E_{0,1} \approx 2(b/J)^3/3$ (see inset of Fig. 1). This confirms the above semiclassical considerations in terms of tunnel doublets. Moreover, we see that the g.s. can only approximate a GHZ state although this approximation will turn out to be very good even at finite temperatures where mixing with excited states additionally decreases the entanglement. Before discussing this in greater detail, we study the ground-state of the general anisotropic case with $J_{xy} \neq J_z$ in the Hamiltonian (1).

When $J_{xy} \neq J_z$ it is possible to generate highly entangled states by applying a spatially uniform magnetic field either perpendicular to or in the xy -plane. Indeed, a field along the z -axis, i.e., $\mathbf{b}_i = b\mathbf{e}_z$, $i = 1, 2, 3$, with $b > 0$ yields an exact W state as g.s. if $J_{xy} > 0$ and $b < J_{xy} - J_z$ (note that this implies the condition $J_{xy} > J_z$). The optimal Zeeman energy b_{opt} leading to the highest energy splitting ΔE_{opt} between the g.s. and the first excited state is given by $b_{\text{opt}} = (J_{xy} - J_z)/2$. This yields $\Delta E_{\text{opt}} = 3J_{xy}/2$ if $J_z < -2J_{xy}$ and $\Delta E_{\text{opt}} = (J_{xy} - J_z)/2$ otherwise. The W state is thus best realized by choosing $b = b_{\text{opt}}$ together with a temperature sufficiently small compared to ΔE_{opt} . In order to obtain a GHZ state, one has to apply an in-plane magnetic field $\mathbf{b}_i = b\mathbf{e}_x$. In

this case we find for $J_z > 0$, $-2J_z < J_{xy} < J_z$ a situation similar to the one in the case of isotropic coupling and radial magnetic field: The g.s. converges to a GHZ state for vanishing field but also the energy difference to the first excited state goes to zero in this limit.

Entanglement measure.— Below, we will quantitatively study the effects of finite temperature $T > 0$ on the amount of entanglement present in the system. For this purpose, we evaluate a suitable mixed-state EM of the canonical density matrix ρ of the system. The three-tangle, or simply *tangle* τ_p (originally called residual entanglement), is an EM for pure states $|\psi\rangle \in \mathcal{H}_1 \otimes \mathcal{H}_2 \otimes \mathcal{H}_3$ of three qubits. It reads [11]

$$\tau_p(|\psi\rangle) = 4 \det \text{Tr}_{2,3} \rho_p - \mathcal{C}^2(\text{Tr}_3 \rho_p) - \mathcal{C}^2(\text{Tr}_2 \rho_p), \quad (3)$$

where $\rho_p = |\psi\rangle\langle\psi|$, Tr_i denotes the partial trace over subsystem i , and \mathcal{C} is the two-qubit concurrence [18]. The tangle takes values between 0 and 1 and is maximal for GHZ states. It is also known that τ_p is an entanglement monotone [3]. The generalization of pure-state monotones to mixed states is given by the so-called convex roof [9, 14, 19]. Accordingly, the mixed-state tangle τ is defined as

$$\tau(\rho) = \inf_{\{p_i, |\psi_i\rangle\} \in \mathfrak{D}(\rho)} \sum_i p_i \tau_p(|\psi_i\rangle). \quad (4)$$

Here, $\mathfrak{D}(\rho)$ denotes the set of all pure-state decompositions $\{p_i, |\psi_i\rangle\}_{i=1}^K$ of ρ , with $\sum_{i=1}^K p_i |\psi_i\rangle\langle\psi_i| = \rho$, $p_i \geq 0$, $\sum_{i=1}^K p_i = 1$ and $K \geq R = \text{rank } \rho$. The above definition of τ ensures that $\tau(\rho) = \tau_p(|\psi\rangle)$ if $\rho = |\psi\rangle\langle\psi|$, and that τ itself is an entanglement monotone [9].

Numerical evaluation.— In order to tackle the optimization problem in Eq. (4) numerically, the set of all pure-state decompositions $\mathfrak{D}(\rho)$ needs to be given in an explicitly parameterized form. It is known [20, 21] that every pure state decomposition $\{p_i, |\psi_i\rangle\}_{i=1}^K$ of ρ is related to a complex $K \times R$ matrix U satisfying the unitary constraint $U^\dagger U = \mathbf{1}_{R \times R}$, i.e., a matrix having orthonormal column vectors [22]. In fact, the set of all such matrices, the so-called Stiefel manifold $St(K, R)$, provides a complete parametrization of all pure-state decompositions $\{p_i, |\psi_i\rangle\}_{i=1}^K \in \mathfrak{D}(\rho)$ of ρ with fixed cardinality K . The minimization problem in Eq. (4) can thus be rewritten as

$$f(\rho) = \min_{K \geq R} \inf_{U \in St(K, R)} h(U, \rho), \quad (5)$$

where in our case h is the sum over the weighted pure-state tangles with probabilities and state vectors obtained from ρ via the matrix U . Problems of this kind are considered to be extremely difficult to solve in general [8]. We have performed the minimization over the Stiefel manifold numerically using the method described below. We have found that the thereby obtained values converge quickly as K is increased, and have thus fixed

$K = R + 4$ throughout all of our calculations, yielding an accuracy which is by far sufficient for our purpose (note that decompositions with smaller cardinality are contained as well). The numerical method we used is a generalization of the conjugate gradient algorithm presented in Ref. [13]. It is however only suited for searching over the unitary manifold $St(K, K)$. At the cost of over-parameterizing the search space, we have to minimize over $K \times K$ matrices using only the first R columns. The iterative algorithm builds conjugate search directions X (skew-hermitian $K \times K$ matrices) from the gradient G at the current iteration point U and the previous search direction using a modified Polak-Ribière update formula. A line search along the geodesic $g(t) = U \exp(tX)$ going through U in direction X is performed in every step. In Ref. [13], an analytical expression for the gradient G is given in the case where f is the EOF. The algorithm is however also applicable to a generic convex-roof EM f of the form (5). We find the matrix elements G_{jk} of the general gradient G to be

$$G_{jk} = (A_{jk} - A_{kj})/2 + i(S_{jk} + S_{kj})/2, \quad (6)$$

where

$$A_{jk} = \sum_{i=1}^K \left(\frac{\partial h}{\partial \text{Re} U_{ik}} \text{Re} U_{ij} + \frac{\partial h}{\partial \text{Im} U_{ik}} \text{Im} U_{ij} \right), \quad (7)$$

$$S_{jk} = \sum_{i=1}^K \left(\frac{\partial h}{\partial \text{Im} U_{ik}} \text{Re} U_{ij} - \frac{\partial h}{\partial \text{Re} U_{ik}} \text{Im} U_{ij} \right). \quad (8)$$

The derivatives of h with respect to the real and imaginary parts of U_{ik} , $\text{Re} U_{ik}$ and $\text{Im} U_{ik}$, respectively, are taken at U and can be evaluated numerically using finite differences. We have tested our implementation by comparing our numerical results to known analytical results. The maximal encountered absolute error was smaller than 10^{-13} for the EOF of isotropic 2×2 states [23], 10^{-12} for 3×3 states and 10^{-10} for the tangle of a GHZ/W mixture [19]. This suggests that, although our method can only provide an upper bound, this bound is very tight. It was shown only recently that also a (typically tight) lower bound on any entanglement monotone can be estimated using entanglement witnesses [24, 25]. This is an interesting subject which is left for future research.

Finite temperature.— We return to the study of the three qubits described by the Hamiltonian (1). Using the generalized conjugate gradient algorithm, we are able to investigate the entanglement as a function of the temperature T , the magnetic field strength b and the exchange couplings J_{xy} and J_z by calculating the mixed-state tangle $\tau(\rho)$, where $\rho = \exp(-H/k_B T)/\text{Tr} \exp(-H/k_B T)$ is the canonical density matrix of the system. To our knowledge, this is the first time that $\tau(\rho)$ has been evaluated for states arising from a physical model. Our main goal now is to maximize the entanglement as a function of

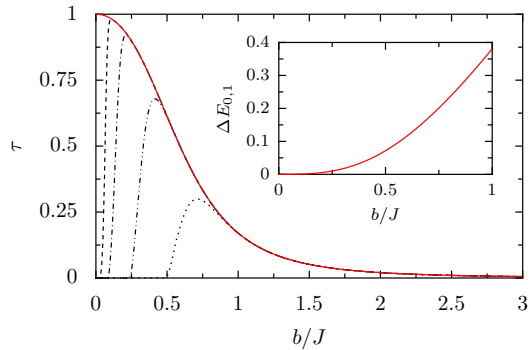


FIG. 1: (color online) The tangle τ of the system with isotropic positive (ferromagnetic) coupling J and radial magnetic field as a function of b/J for different temperatures $T = 10^{-4} J/k_B$ (dashed line), $10^{-3} J/k_B$ (dash-dotted line), $10^{-2} J/k_B$ (dash-dot-dotted line) and $5 \times 10^{-2} J/k_B$ (dotted line). Note the twofold influence of the temperature on τ : Although higher temperatures reduce the maximally achievable entanglement, a stabilizing effect is observed as well. A maximum in the tangle is more robust against fluctuations in b at higher temperatures due to the less rapid drop-off of τ as b/J is reduced. Conversely, τ of the approximate GHZ g.s. |GS> ($T = 0$, red line) shows a discontinuity at $b = 0$, where $\tau(\rho) = 0$. For $b > 0$, we find the simple algebraic expression $\tau_p(|GS\rangle) = (3 - 8b/J)/C + 2/\sqrt{C}$, where $C = 9 + 4b(4b/J - 3)/J$. Inset: Energy splitting $\Delta E_{0,1}$ of the ground-state doublet as a function of b/J .

$b \equiv |b_i|$, i.e., the Zeeman energy. For this purpose we consider only GHZ states in the following, since our W ground states are b -independent (see above). In the system with isotropic exchange coupling $J > 0$ and radial magnetic field, the tangle τ tends to zero for $b/J \rightarrow 0$ due to the vanishing energy splitting $\Delta E_{0,1}$ (see Fig. 1). We remark that this behavior is discontinuous at $T = 0$, where $\tau(\rho) \rightarrow 1$ for $b/J \rightarrow 0$, but $\tau(\rho) = 0$ at $b = 0$. With larger b/J , the g.s. contributes dominantly to ρ but simultaneously deviates increasingly from a GHZ state. The entanglement in the system is therefore reduced (cf. solid line in Fig. 1). For a given temperature, the maximal tangle τ_{\max} is therefore obtained at a finite optimal value $(b/J)_{\text{opt}}$ of the scaled magnetic field strength as a trade-off between having a highly entangled g.s. and separating the latter from excited states in order to avoid the negative effects of mixing. For low temperatures $T \lesssim 10^{-2} J/k_B$, we numerically find the power laws $(b/J)_{\text{opt}} \propto (k_B T/J)^\alpha$ and $1 - \tau_{\max} \propto (k_B T/J)^\beta$ with the exponents $\alpha \approx 0.30$ and $\beta \approx 0.63$. Specifically, we obtain $\tau(\rho) = 0.98$ (0.92) for $T = 10^{-4} J/k_B$ ($10^{-3} J/k_B$) and $b = 0.11J$ ($0.21J$). Apart from the effect of reducing τ_{\max} , finite temperatures also possess the advantageous feature of broadening the discontinuity of τ at $T = 0$ and $b = 0$ which makes τ_{\max} more stable against fluctuations of b around b_{opt} (see Fig. 1).

We finally come back to the general anisotropic

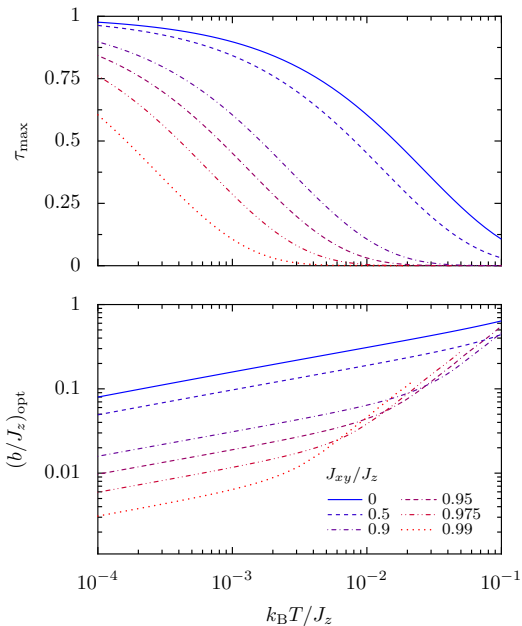


FIG. 2: (color online) Top: Maximally achievable tangle τ_{\max} in the anisotropic system (GHZ g.s.) with homogeneous in-plane magnetic field and $J_z > 0$ as a function of temperature for six anisotropy ratios J_{xy}/J_z (see legend). The curves end at $\tau(\rho) = 10^{-5}$. Bottom: The corresponding optimal values $(b/J_z)_{\text{opt}}$ of the scaled magnetic field strength b/J_z .

model (1) with $J_{xy} \neq J_z$ subject to a homogeneous in-plane magnetic field. In Fig. 2 we show the maximally achievable tangle τ_{\max} (optimized with respect to b/J_z) as a function of temperature for various anisotropy ratios J_{xy}/J_z (where, as before, $J_z > 0$). Since we are interested in high values of τ_{\max} , an arbitrary but low cutoff was introduced in the calculation at $\tau(\rho) = 10^{-5}$. The lower panel of Fig. 2 depicts the corresponding optimal field values $(b/J_z)_{\text{opt}}$. At low temperatures T , a power-law dependence of $(b/J_z)_{\text{opt}}$ on T is observed, similar to the above isotropic case. Note that a higher amount of entanglement can be realized in systems with stronger anisotropies. E.g., for Ising coupling ($J_{xy}/J_z = 0$) we find $\tau(\rho) = 0.98$ (0.89) for $T = 10^{-4}J/k_B$ ($10^{-3}J/k_B$) and $b = 0.080J_z$ ($0.16J_z$). At $T = 10^{-4}J/k_B$ but with $J_{xy}/J_z = 0.9$, still a very good value $\tau(\rho) = 0.90$ is achieved for $b = 0.016J_z$. We remark that still higher tangles are obtained for negative (antiferromagnetic) $J_{xy} > -2J_z$. In this case, the maximal tangle as a function of T decays even more slowly than the curves displayed in the top panel of Fig. 2.

Possible implementations of the qubits include GaAs and InAs quantum dots, InAs nanowires or single-wall carbon nanotubes. Assuming a typical value of $|J| \sim 1$ meV [26, 27] we obtain $\tau \approx 0.9$ at $T \approx 10$ mK and $B \approx 2$ T (assuming a g -factor of $|g| = 2$). Ferromagnetic coupling is achieved by operating the dots with more than one electron per dot.

We thank D. Bulaev, G. Burkard, L. Chirolli, W.A. Coish, and D. Stepanenko for useful discussions. Financial support by the EU RTN QuEMolNa, the EU NoE MAGMANet, the NCCR Nanoscience, and the Swiss NSF is acknowledged.

-
- [1] A. Einstein, B. Podolsky, and N. Rosen, *Phys. Rev.* **47**, 777 (1935); J. Bell, *Physics* **1**, 195 (1964); A. Aspect, P. Grangier, and G. Roger, *Phys. Rev. Lett.* **49**, 91 (1982); R. F. Werner, *Phys. Rev. A* **40**, 4277 (1989).
 - [2] D. M. Greenberger, M. Horne, and A. Zeilinger, *Bell's Theorem, Quantum Theory, and Conceptions of the Universe* (Kluwer Academic Publishers, Dordrecht, 1989).
 - [3] W. Dür, G. Vidal, and J. I. Cirac, *Phys. Rev. A* **62**, 062314 (2000).
 - [4] M. A. Nielsen and I. L. Chuang, *Quantum Computation and Quantum Information* (Cambridge University Press, New York, 2000).
 - [5] R. Raussendorf, D. E. Browne, and H. J. Briegel, *Phys. Rev. A* **68**, 022312 (2003).
 - [6] S. Bose, *Phys. Rev. Lett.* **91**, 207901 (2003).
 - [7] A. K. Rajagopal and R. W. Rendell, *Phys. Rev. A* **65**, 032328 (2002).
 - [8] M. B. Plenio and S. Virmani, *Quant. Inf. Comp.* **7**, 1 (2007).
 - [9] F. Mintert *et al.*, *Phys. Rep.* **415**, 207 (2005).
 - [10] C. H. Bennett *et al.*, *Phys. Rev. A* **54**, 3824 (1996).
 - [11] V. Coffman, J. Kundu, and W. K. Wootters, *Phys. Rev. A* **61**, 052306 (2000).
 - [12] T.-C. Wei and P. M. Goldbart, *Phys. Rev. A* **68**, 042307 (2003).
 - [13] K. Audenaert, F. Verstraete, and B. De Moor, *Phys. Rev. A* **64**, 052304 (2001).
 - [14] A. Uhlmann, *Phys. Rev. A* **62**, 032307 (2000).
 - [15] Depending on the actual implementation of the qubits, \mathbf{b}_i can denote an effective magnetic field.
 - [16] Using semiclassical path integration techniques [17], we can calculate the tunnel splitting from Eq. (2). However, such a procedure gives accurate results only for large spins ($S \gg 1$) and is thus not pursued here.
 - [17] D. Loss, D. P. DiVincenzo, and G. Grinstein, *Phys. Rev. Lett.* **69**, 3232 (1992).
 - [18] W. K. Wootters, *Phys. Rev. Lett.* **80**, 2245 (1998).
 - [19] R. Lohmayer *et al.*, *Phys. Rev. Lett.* **97**, 260502 (2006).
 - [20] L. P. Hughston, R. Jozsa, and W. K. Wootters, *Phys. Lett. A* **183**, 14 (1993).
 - [21] K. A. Kirkpatrick, *Found. Phys. Lett.* **19**, 95 (2005).
 - [22] Given ρ and U with $U^\dagger U = \mathbb{1}_{R \times R}$, $\{p_i, |\psi_i\rangle\}_{i=1}^K$ is obtained as $p_i = \langle \tilde{\psi}_i | \tilde{\psi}_i \rangle$, $|\psi_i\rangle = (1/\sqrt{p_i})|\tilde{\psi}_i\rangle$, where $|\tilde{\psi}_i\rangle = \sum_{j=1}^R U_{ij} \sqrt{\lambda_j} |\chi_j\rangle$ and $|\chi_i\rangle$ are the R eigenvectors of ρ with non-zero eigenvalues λ_i .
 - [23] B. M. Terhal and K. G. H. Vollbrecht, *Phys. Rev. Lett.* **85**, 2625 (2000).
 - [24] O. Gühne, M. Reimpell, and R. F. Werner, *Phys. Rev. Lett.* **98**, 110502 (2007).
 - [25] J. Eisert, F. G. S. L. Brandão, and K. M. R. Audenaert, *New J. Phys.* **9**, 46 (2007).
 - [26] V. Cerletti *et al.*, *Nanotechnology* **16**, R27 (2005).
 - [27] R. Hanson *et al.*, *Rev. Mod. Phys.* **79**, 1217 (2007).